Bamboo charcoal derived high-performance activated carbon via microwave irradiation and KOH activation: application as hydrogen storage and super-capacitor

Xiuying Fang[a,†], Guizhen Li[a,†], Jiaxiong Li[a], Hai Jin[a], Jianmin Li[a], Veeriah Jegatheesan[b], Shu Li[b], Hongbin Wang[a,*], Min Yang[a,*]

[a]*School of Chemistry and Environment, Yunnan Minzu University, Kunming, Yunnan 650500, China,*
emails: 595530820@qq.com (H. Wang), 826677468@qq.com (M. Yang), 1197084904@qq.com (X. Fang),
325865775@qq.com (G. Li), 243990-096@qq.com (J. Li), 1641684392@qq.com (H. Jin), 1462265356@qq.com (J. Li)
[b]*School of Civil, Environmental and Chemical Engineering, RMIT University, Melbourne VIC 3000, Australia,*
emails: li.shu@rmit.edu.au (L. Shu), jega.jegatheesan@rmit.edu.au (V. Jegatheesan)

abstract

This paper attempts to prepare high-performance activated carbon (HP-AC) from bamboo charcoal (BC) as raw material using microwave irradiation as heating source and potassium hydroxide as activating agent. The influence of factors, such as activation time (3–15 min), KOH/C ratio (1:1–6:1) and particle size (0.147–2 mm) on its performance (the carbon yield and adsorptive capability) were investigated. The textural porosity and surface chemistry of HP-AC were determined by scanning electron microscope (SEM) analyzer, N_2 adsorption method and Fourier-transform infrared (FT-IR) spectrometer. The adsorptive properties of HP-AC were examined using iodine solution and methylene blue as model dye compound and hydrogen adsorbate. The effect of porosity and surface functionalities on the electrochemical capacitance of HP-AC were measured by cyclic voltammetry measurements. Under the best preparation conditions (activation time of 8 min, KOH/C ratio of 5:1 and particle size of 0.71–1.4 mm), the following results were obtained for the specific surface area, micro surface area, external surface area, total pore volume, iodine adsorption value, methylene blue adsorption value, carbon yield, hydrogen storage capacity and super capacitance value: 2,446 m^2/g, 901 m^2/g, 1,545 m^2/g, 1.48 mL/g, 2,226 mg/g, 47.5 mL/0.1 g, 34.3%, 0.93 wt% (17.3 MPa, 25°C) and 3.63 wt% (1.0 MPa, −196°C), 212 F/g, respectively. The findings revealed the potential of BC as a raw material for the preparation of HP-AC, and to determine its potential applications of HP-AC as hydrogen storage and super-capacitor material.

Keywords: Microwave irradiation; High-performance activated carbon; Hydrogen storage; Super capacitance; KOH

1. Introduction

High-performance activated carbon (HP-AC) is a carbonaceous material, which has special crystalline structure, abundant surface functional groups, large specific surface area and good adsorptive performance [1]. With the continuous development of modern industries, HP-AC has been widely used in chemical industry, environmental protection, food, medical appliances, solvent recovery, water treatment, fuel cells, gas storage, hydrometallurgy, military chemical protection and other fields, which become indispensable

---

* Corresponding author.

† These two authors contributed equally to this work.

products of the national economy, national defense construction and people's daily life indispensable products.

Up to date, physical (water vapor, CO_2, etc.), chemical (KOH, $ZnCl_2$, K_2CO_3, H_3PO_4, etc.) and composite activation are used for the preparation of HP-AC [2,3]. Both chemical and physical activations have their advantages and disadvantages. Chemical activation for the preparation of HP-AC have developed internal pores and increased large specific surface area, but this method led to serious equipment corrosion and waste water treatment. Further, the recycling of activators is difficult. Although the specific surface area is less by the physical activation, its advantages are that the process of activation does not produce pollution and the products are formed without pickling and washing. There are two heating methods for the preparation of HP-AC [4], traditional thermal heating method (high temperature resistance furnace heating) and new type of heating method (microwave radiation heating). Traditional thermal heating method transfers power from external to internal with small heating rates and therefore the internal temperature of the material is not uniform. Compared with the traditional thermal heating method, microwave radiation is from the internal spreading to the outside and therefore the microwave radiation has the advantages of large heating rates, uniform heating of materials and shorter time of activation [5]. Thus, the method of using microwave heating and KOH activation, which take shorter time in the whole activation stage, can help to prepare HP-AC that exhibits the characteristics of high-efficiency and save energy.

At present, hydrogen storage methods liquefy the hydrogen under high pressure, which has high risk coefficient and high requirement on the equipment. Carbon material adsorption is one of the best methods of hydrogen storage [6], because the HP-AC has many merits including good adsorption ability, well developed pore structure and great specific surface area. The percentage of hydrogen storage mass is 7.4 wt% with HP-AC made by Li Zhou as a hydrogen storage material at 77 MPa and had exceeded the international standard (5 wt%). It shows that HP-AC has a great prospect in the field of hydrogen storage. Making the capacitor electrode material with the HP-AC using KOH (3 mol/L) as the electrolyte solution, the specific capacitance of the electrode materials was 369 and 305 F/g at the current densities of 50 and 2,500 mA/g, respectively [7]. After cycling 1,000 times, the specific capacitance of AC was still relatively high and could be maintained above 92%, which indicates that HP-AC has great value in the application and development of super capacitor electrode materials.

Therefore, we attempted to produce HP-AC from bamboo charcoal (BC) by microwave irradiation with KOH activation and the factors such as activation time, KOH/C ratio and particle size were explored systematically.

2. Methods

2.1. Evaluation for the preparation of HP-AC

The molecular structure of iodine and methylene blue were I_2 and $C_{16}H_{18}N_3SCl$, respectively, which were purchased in Tianjin wind boat Chemical Reagent Technology Co. and were selected as the model adsorbents. The optimum conditions of the activation time, KOH/C ratio and particle size for the preparation of AC were determined by iodine and methylene blue values.

2.2. The preparation of HP-AC

Bamboo charcoal purchased in Tianjin wind boat Chemical Reagent Technology Co., and its iodine adsorption value was 148 mg/g, which was mixed with KOH (Chemical Reagent Technology Co., Tianjin) and water; different KOH/C ratios were selected (1:1, 2:1, 3:1, 4:1, 5:1 and 6:1) and a timer was used for various exposure times (3, 5, 8, 10, 12 and 15 min). This mixer was dried in an oven and put the resultant into a microwave oven and activated under the power of 800 W. The resultant was washed with 0.1 mol/L hydrochloric acid and rinsed repeatedly with water until the pH value was about 7. Finally, the products were obtained by the processes of rinsing 2–3 times with deionized water, and dried in the oven at 120°C.

2.3. Characterization of activated carbon

The chemical characterization of surface functional groups of HP-AC was obtained by Fourier-transforms infrared (FTIR) spectroscopy (Nicolet, Is10). The porous structures of HP-AC determined by nitrogen (N_2) adsorption–desorption isotherm at 77 K using automatic volumetric adsorption analyzer. The specific surface area was calculated by the Brunauer–Emmett–Teller (BET) equation. The total pore volume was evaluated by converting the adsorption volume of nitrogen at relative pressure of 0.98 to equivalent liquid volume of adsorbate. The microspore volume, microspore surface area and external surface area were deduced using the *t*-plot method. The surface morphologies were examined by a scanning electron microscope (SEM). The crystalline structures of HP-AC were analyzed by X-ray diffraction (XRD). The mass loss of HP-AC was explored by thermogravimetric (TG) and differential thermal analysis (DTA). Hydrogen absorption–desorption properties of HP-AC were determined by hydrogen adsorption–desorption isotherm at 25°C and −196°C using an automatic micrometrics 3H-2000P-H1 volumetric adsorption analyzer.

3. Results and discussions

3.1. The preparation of HP-AC from BC

3.1.1. Effects of activation time

The experiment was carried out at different activation time (3, 5, 8, 10, 12 and 15 min) with a microwave power of 800 W and a particle size ranging from 0.71 to 1.4 mm. A 1:1 molar ratio of KOH/C was used for 10 g of BC samples. The effect of activation time on the carbon yield, iodine and methylene blue adsorption value is shown in Table 1. It can be seen that the iodine and methylene blue adsorption value of HP-AC showed a sharp growth, which increased from 768 to 1,199 mg/g and 8.7 to 19 mL/0.1 g, respectively, with prolonging the microwave radiation time from 0 to 8 min. Afterwards, the adsorbed value decreased from 1,199 to 1,117 mg/g, and then steadily decreased further. It reveals clearly that the reaction was carried out fully and formed the pore network when the activation time was prolonged.

The above was probably due to the sintering effect, which significantly destroyed the pore walls between the adjacent pores, resulted in the formation of mesopores or megalopores by excessive reaction as. Higher pyrolysis temperatures could induce to

produce C–KOH, C–K$_2$CO$_3$, C–K, C–K$_2$O, C–CO and C–CO$_2$ [8]. Reactions facilitating breakage of the C–O–C and C–C bonds thus the variation of the carbon yield had a decreasing trend. In addition, further heat treatment may produce local hotspots, leading to the ablation and contraction of carbon internal channels. Therefore, 8 min was selected as the best activation time.

3.1.2. Effects of KOH/C ratio

The effects of the KOH/C ratio were studied through activation using KOH as an activator for 8 min at a microwave power of 800 W and different KOH/C ratios ranging from 1:1 to 6:1. The experimental results are shown in Table 2. The results showed that the iodine adsorption value enhanced from 1,199 to 2,196 mg/g with the increase of KOH/C ratio from 1:1 to 5:1 and then decreased from 2,196 to 1,998 mg/g when the KOH/C ratio was increased from 5:1 to 6:1. There was a drastic increase of methylene blue adsorption value from 19 to 40.5 mg/0.1 g with the KOH/C ratio increased from 1:1 to 5:1 and then decreased. There was a gradual decrease of carbon yield with the increase of KOH/C ratio from 1:1 to 6:1. This shows that the activating reaction rate was increased with the increase of KOH.

Obviously, the development of porosity was related to gasification of KOH. The metallic potassium formed during the gasification process would diffuse into the internal structure of the BC matrix expanding the existing pores and creating new pores [9]. Thus, the activation process would be enhanced by increasing of KOH/C ratio. Correspondingly, the adsorption capacity will be improved further. The active sites on C reacted fully at the KOH/C ratio of 5:1 and the adsorption capacity reached to its maximum. Exceeding the optimum will cause excessive reaction during which the micropores would be broadened and burned, further forming mesopores and macropores, thereby reducing the adsorption capacity and yield of HP-AC. Therefore, it was recommended that the KOH/C ratio of 5:1 to be used in the preparation of HP-AC.

3.1.3. Effects of particle size

Samples with different particle size of BC (1.4–2, 0.71–1.4, 0.25–0.71, 0.147–0.25 mm and less than 0.147 mm) were made and activated under the following conditions: KOH/C ratio (5:1), activation time (8 min) and microwave power (800 W). Table 3 presents the results of the experiments. Obviously, the highest iodine adsorption value was 2,226 mg/g when the particle size was 0.71–1.4 mm, and then had a decreasing trend with the particle size less than 0.147. The methylene blue adsorption values of HP-AC had a tendency to increase slowly.

It is clear that the particle size of BC had weak correlation as the activating reaction basically occurred on the surface of BC; the internal activation of AC was not sufficient and the contact of activator with BC surface was large which led to excessive activation of BC. The BCs internal micropores were expanded to form mesopores or macropores resulted in the decrease of micropores and therefore increasing the medium and large pores and decreasing the iodine value.

3.2. The characterization of HP-AC

3.2.1. Infrared analysis of HP-AC

The FTIR spectra of BC and HP-AC are presented in Fig. 1. By comparing the FTIR spectra, we can see only little

Table 1
Effect of the activating time (experimental conditions: microwave power of 800 W, particle size of 0.71–1.4 mm, KOH/C ratio of 1:1, mass of 10 g)

Activation time (min)	3	5	8	10	12	15
Iodine adsorption value C_0 (mg/g)	148	148	148	148	148	148
Iodine adsorption value C (mg/g)	746	844	1,199	1,158	1,095	1,117
Methylene blue adsorption value (mL/0.1 g)	8.3	12.7	19.0	18.4	15.1	17.2
Carbon yield (%)	57.1	52.6	49.4	47.3	42.8	40.2

Table 2
Effect of KOH/C ratio (experimental conditions: microwave power of 800 W, particle size of 0.71–1.4 mm, activation time of 8 min, mass of 10 g)

KOH/C ratio (g)	1:1	2:1	3:1	4:1	5:1	6:1
Iodine adsorption value C_0 (mg/g)	148	148	148	148	148	148
Iodine adsorption value C (mg/g)	1,199	1,474	1,576	1,960	2,196	1,998
Methylene blue adsorption value (mL/0.1 g)	19.0	24.5	27.6	37.4	40.5	38.2
Carbon yield (%)	49.4	42.6	40.0	38.1	35.2	30.2

Table 3
Effect of the particle size (experimental conditions: microwave power of 800 W, activation time of 8 min, KOH/C ratio of 5:1, mass of 10 g)

Particle size (mm)	1.4–2	0.71–1.4	0.25–0.71	0.147–0.25	<0.147
Iodine adsorption value C_0 (mg/g)	148	148	148	148	148
Iodine adsorption value (mg/g)	2,196	2,226	2,225	2,150	2,104
Methylene blue adsorption value (mL/0.1 g)	40.5	44	41.5	42.6	43
Carbon yield (%)	35.2	34.3	32	31.8	28.3

differences in chemical composition on the surface of HP-AC and BC, and all the spectra had similar adsorption peaks. There were four major peaks at about 3,450, 1,440, 1,068, 860 cm^{-1}, which suggested the existence of –OH, C=C (aromatic ring), C–O–C and C–H (aromatic ring) stretching. From the FTIR spectra, it can be known that the peak had a decreasing tendency at 3,450 cm^{-1} and it would come from the pyrolysis of radical groups, which led to the decrease of hydroxylate in activation process with high temperature. Moreover, the peak areas have little difference at about 1,440, 1,070 and 860 cm^{-1}, which indicates that it is hard to change the surface functional groups naturally but easy to change its physical properties.

3.2.2. The BET characterization of HP-AC

It can be seen from Fig. 2 that density functional theory (DFT) model ascertained the pore size distribution of HP-AC. The result shows that the micropores were mainly concentrated at 0.504, 0.889 and 1.29 nm, the distribution of the mesopores was concentrated at 3.09, 5.18, 6.16 and 7.06 nm, and the sharpest peak occurred at pore diameters between 0.889 and 3.09 nm, which shows that a vast majority of the pores fell into the mesopore range. Fig. 3 shows the micropore size distribution where the sharpest peak occurred at pore diameters from 0.3 to 0.9 nm. Ultra-micropores had a larger proportion in the particle size distribution. The result was consistent with iodine adsorption curve [10]. The DFT analysis also shows that HP-AC specific surface area, total pore volume, micropore surface area and external surface area were 2,446.22 m^2/g,

1.480 mL/g, 901 m^2/g and 1,545 m^2/g, respectively (see Table 4). In short, the pore size distribution of HP-AC was consistent with Langmuir adsorption isotherm.

3.2.3. SEM analysis of HP-AC

We observed the porous structure of BC and HP-AC with magnification 60,000× by SEM. Fig. 4 shows the surface morphology of BC and HP-AC. Fig. 4(a) exhibits that the surface structures of BC was relatively smooth. After activation, as can be seen from Fig. 4(b), it is clear that the HP-AC formed a considerable number of pores, so it had a large specific surface area which was consistent with the high iodine adsorption value and BET [11].

3.2.4. XRD analysis of the crystalline structure of HP-AC

According to Fig. 5, we found BC and HP-AC had two obvious characteristic peaks, which were around 2θ = 25° and 2θ = 43° [12], respectively. The two peaks were diffraction peaks of HP-AC (002 and 100) [13]. Normally, when the heating temperature gets higher, the crystallite structure of carbon containing materials would be changed, so that the intensity of the diffraction characteristic peaks of the crystallite increased. As could be seen from the diagram, the strength of HP-AC (100) peak was much greater than the strength of BC, which shows HP-AC had more crystallites than BC.

3.2.5. TG-DSC analysis of the thermal behavior and weight loss of HP-AC

The TG-differential scanning calorimetry (DSC) curve of HP-AC and BC are shown in Figs. 6 and 7. More detailed discussions on this can be found elsewhere [14]. The mass loss
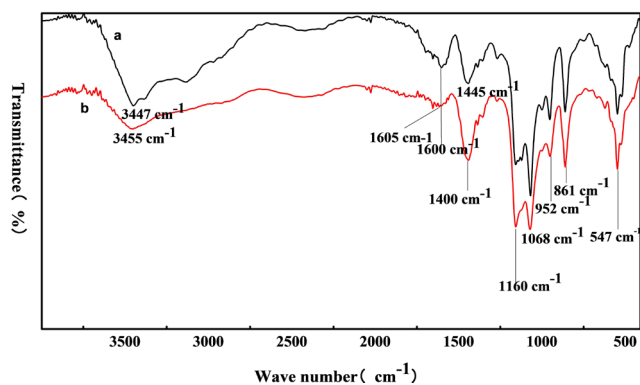
Fig. 1. FTIR of BC (a) and HP-AC (b).
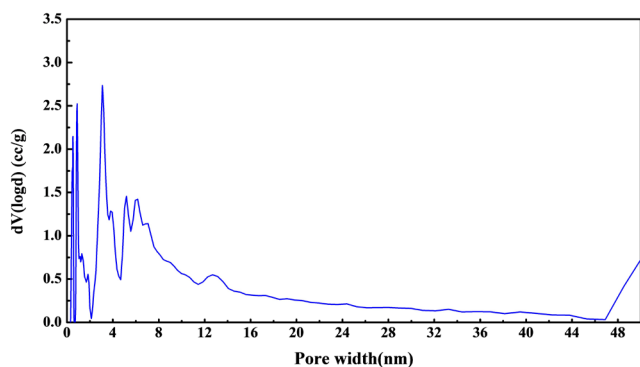
Fig. 2. Pore size distribution of HP-AC.
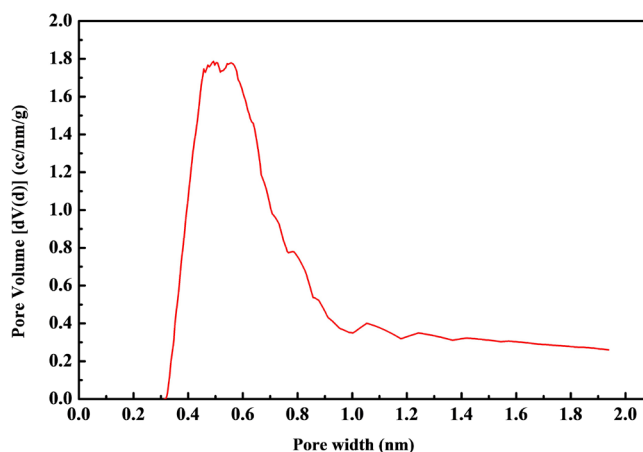
Fig. 3. Micropore size distribution of HP-AC.

Table 4
Porosity structure and surface properties of HP-AC

Specific surface area (m^2/g)	2,446.22
Total pore volume (mL/g)	1.480
Micropore surface area (m^2/g)	901
External surface area (m^2/g)	1,545
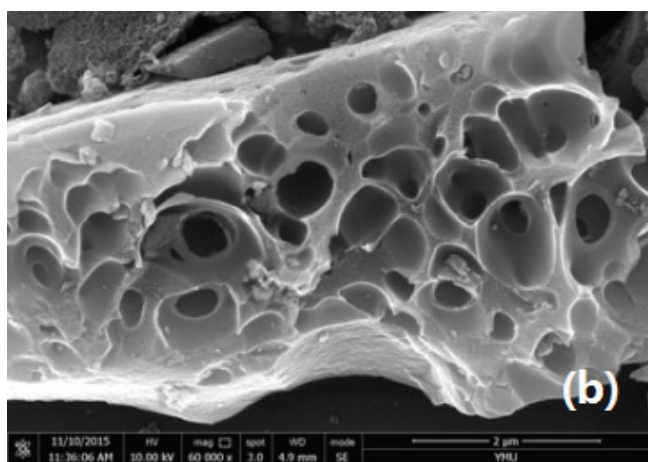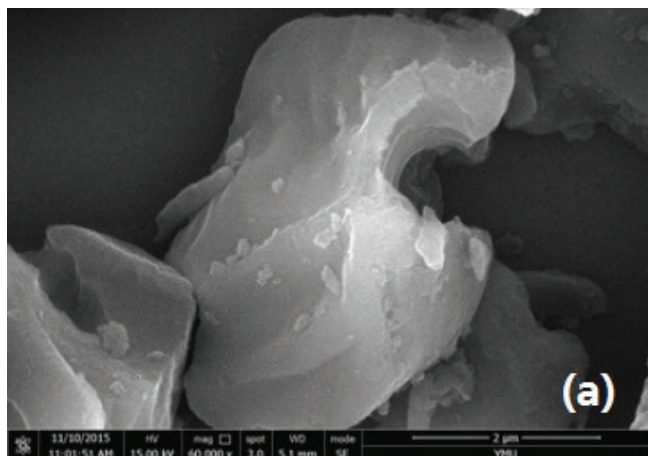
Fig. 4. SEM micrograph of: BC (a) and HP-AC (b) with magnification 60,000×.
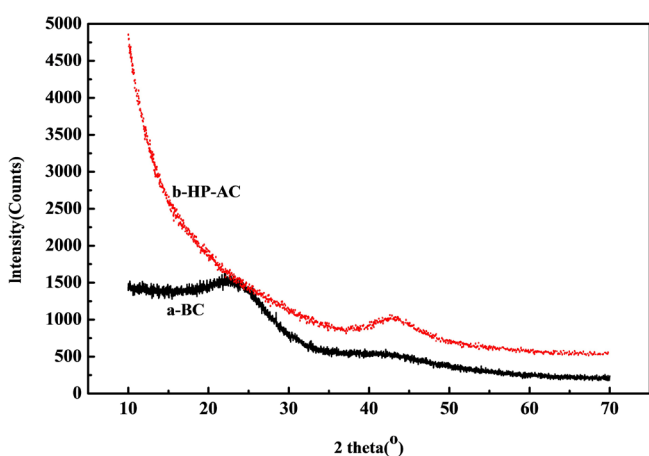
Fig. 5. XRD of: BC (a) and HP-AC (b).

was more obvious when the temperature was increased from 20°C to 100°C (the mass loss of HP-AC and BC were about 19% and 3%, respectively), that was mainly caused by moisture in the carbon material evaporation and there were abundant pore structures after activation which can absorb large
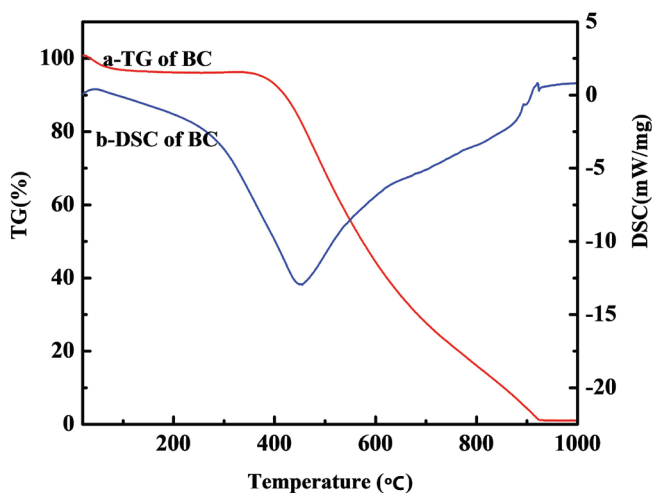
Fig. 6. Characteristic curves of BC: TG (a) and DSC (b).
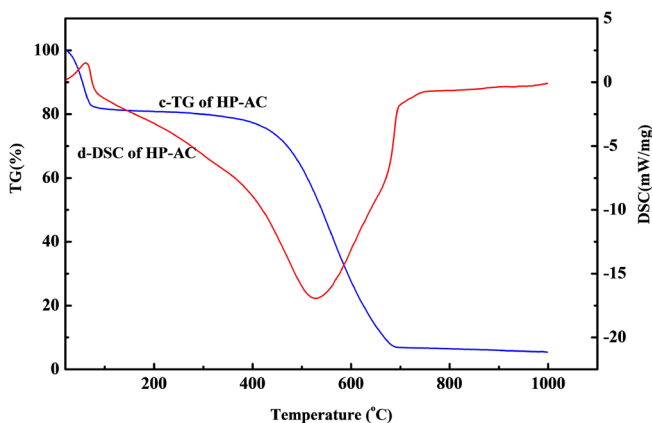
Fig. 7. Characteristic curves of HP-AC: TG (c) and DSC (d).

amount of water. The mass loss was about 77% at the second stage when the temperature was increased from 350°C to 700°C; the mass loss in this period was derived from two aspects, one was pyrolysis of the raw material of cellulose and lignin and the other was dehydrogenation reaction of the aromatic compounds which would occur when the temperature over 500°C. The DSC curves of BC and HP-AC had larger endothermic peak between 460°C and 530°C. It indicates that the TG and DSC curves were identical to each other at this temperature range.

3.3. The electrochemical performance test of HP-AC

3.3.1. Hydrogen storage capacity test of HP-AC

Hydrogen storage capacity of HP-AC sample was measured by high pressure physical adsorption instrument at different temperatures. The hydrogen adsorption isotherms of HP-AC are shown in Fig. 8. Obviously, hydrogen storage capacity increased with the increase in pressure at 25°C. Hydrogen storage capacity reached the maximum value of 0.93 wt%, when the pressure reached at 17.3 MPa. At liquid nitrogen temperature (−196°C), hydrogen storage capacity increased at the beginning and reached a stable status;

with the increase of pressure (from 0 to 0.5 MPa), hydrogen storage capacity reached the maximum value of 3.63 wt% (reached 1 MPa).

Table 5 shows the H_2 adsorption rate for AC from different raw materials. It can be seen that the HP-AC possessed similar H_2 adsorption with other AC. Nevertheless, the H_2 adsorption obtained in this study is still inferior compared with that of biomass waste [15]. However, there is no clear standard about H_2 storage capacity and it is still difficult for researchers to find suitable HP-AC to improve H_2 storage capacity. Thus, further study need to improve the H_2 adsorption on HP-AC.

3.3.2. The electrochemical performance test of HP-AC

Figs. 9(a)–(c) exhibit the cyclic voltammetry curves of HP-AC at different scanning rates (100, 50, 10 mV/s). Obviously, the curves are similar to the shapes of the rectangle in organic electrolyte system of LiPF6 (EC+DMC) and there were no obvious oxido-reduction peaks. It suggests that HP-AC form of energy storage was double-layer capacitor. The corresponding peak current increased with the increase of scanning rates which indicates there was no relationship between the specific capacitance and the scanning rate of HP-AC. The capacitor electrode of HP-AC showed good reversible and capacitive characteristics. It also shows that the cyclic voltammetry curves had upward sloping tendency at the corner with different scanning rates; this was mainly due to the electrolyte's chemical decomposition at higher voltage or the effect of the number of mesopores of HP-AC. The oxidation on AC electrode, stabilization, repeatability and gain and lose of electrons were investigated by cyclic voltammetry curves as well as the specific capacitance of capacitor and electrode materials according to corresponding currents. The formula for calculation is as follows:

$$C_P = 4C = 4I/\gamma \times m \times a \qquad (1)$$

(a)

(b)

Fig. 8. Hydrogen adsorption isotherms of HP-AC at: 25°C (a) and −196°C (b).
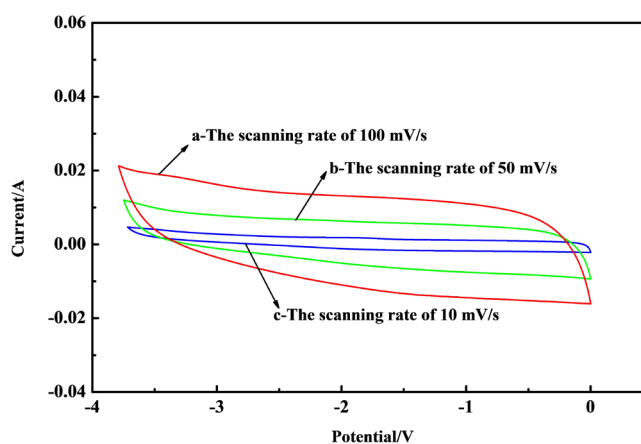
Fig. 9. The cyclic voltammetry curves of HP-AC at different scan rates.

Table 5
Hydrogen adsorption date of ACs from different studies

Feedstock	Surface area, BET (m²/g)	T (K)	P (MPa)	H_2 adsorption (wt%)	References
Commercial-AX-21	3,000	298	6	0.4	[16]
		77	3	5.3	
			7	7.4	
High sulfur petroleum cokes	3,886	293	5	1.9	[17]
		93	6	9.8	
Coffee-shell	3,149	298	6	0.66	[18]
		77	1.1	4.06	
Bamboo charcoal	2,446	293	6	0.54	Present study
		77	1	3.63	

Table 6
Specific capacitance of ACs from different studies

Sample	Surface area, BET (m²/g)	Carbon/acetylene black/adhesive	Electrolyte	C_p (F/g)	References
Commercial AC	2,500	7:2:1	2 mol/L Li₂SO₄ solution (neutral)	129	[19]
Coconut-shell AC	1,700–1,800	8:1:1	6 mol/L KOH solution	360	[20]
Self-made AC	1,920	8:1.5:0.5	1 mol/L KOH solution	206	[21]
Pitch-based AC	2,960	8:1:1	30% KOH solution	198	[22]
			Et₄NBF₄ + PC	93	
HP-AC	2,446	8:1:1	1 mol/L LiPF6 (EC+DMC)	212	Present study

where C_p is the specific capacity (F/g) of a single electrode and C is the specific capacity of the whole capacitor. I (A) is the corresponding current of cyclic voltammetry curve, m (g) is the total mass of double electrode, γ (V/s) is the scan rate and a is the mass fraction of active substrate in the electrode material.

The mass specific capacity of HP-AC electrode material and the specific capacitance of the capacitor were calculated using Eq. (1), which were 212 and 53 F/g, respectively. Table 6 shows the C_p values for AC from different studies. It can be seen that the HP-AC possessed similar C_p value with other AC using different electrolytes. In theory, the surface area has a direct relationship with the energy capacitance [23] which ranged between 69 and 374 F/g [24]. In this regard, HP-AC prepared in this study is a good candidate for super-capacitor applications.

4. Conclusion

This study highlights that the preparation of HP-AC by microwave radiation and KOH activation reduced the heating time and energy consumed as well as decreased cost of preparation. The method showed that HP-AC had an abundant pore structure with the iodine adsorption value of 2,226 mg/g, methylene blue adsorption value of 47.5 mL/0.1 g. It also had a BET surface area of 2,446.22 m²/g, total pore volume of 1.480 mL/g, micropore surface area of 901 m²/g, external surface area of 1,545 m²/g and total pore volume of 0.889 mL/g. The isothermal adsorption of hydrogen by HP-AC was tested at room temperature and liquid nitrogen temperature. The results showed that HP-AC was beneficial when it comes to reduce the pressure of storage devices in the hydrogen storage technology with the hydrogen adsorption value of 0.93 wt% (17.3 MPa, 25°C) and 3.63 wt% (17.3 MPa, −196°C). According to the capacitance performance of HP-AC, it could be used as electrode material with the electrode materials of specific capacity of 212 F/g. All data illustrate that HP-AC has great potential to be used as a capacitor electrode as well as a hydrogen storage material and thus has a great research value for future studies on practical applications.

References

[1] D.J. Kang, X.L. Tang, H.H. Yi, P. Ning, Z.Q. Ye, K. Li, Recent advances in research of super-activated carbon: property, preparation and application, Environ. Sci. Technol., 34 (2011) 110–117.
[2] N. Wei, N.Q. Zhao, W. Jia, New progress in the fabrication and application of activated carbon, Mat. Sci. Eng., 21 (2003) 777–780.
[3] X.Z. Wang, M.Q. Li, Y.X. Ju, Y.L. Zheng, J.H. Wang, Influence of preparation methods on the porosity of activated carbon, Carbon Technol., 6 (2002) 25–30.
[4] Y. Kan, Q. Yue, B. Gao, Q. Li, Comparison of activated carbons from epoxy resin of waste printed circuit boards with KOH activation by conventional and microwave heating methods, J. Taiwan Inst. Chem. Eng., 68 (2016) 440–445.
[5] V.O. Njoku, K.Y. Foo, M. Asif, B.H. Hameed, Preparation of activated carbons from rambutan (*Nephelium lappaceum*) peel by microwave-induced KOH activation for acid yellow 17 dye adsorption, Chem. Eng. J., 250 (2014) 198–204.
[6] T. Adinaveen, L.J. Kennedy, J.J. Vijaya, G. Sekaran, Surface and porous characterization of activated carbon prepared from pyrolysis of biomass (rice straw) by two-stage procedure and its applications in super-capacitor electrodes, J. Mater. Cycles Waste Manage., 17 (2015) 736–747.
[7] B.L. Geng, L.J. Chen, C.X. Zhang, L.Y. Pan, G.H. Huang, Preparation and characterization of activated carbons for super-capacitor under moderate temperature activation condition, J. China Coal Soc., 36 (2011) 1200–1205.

[8] K.Y. Foo, B.H. Hameed, Textural porosity, surface chemistry and adsorptive properties of durian shell derived activated carbon prepared by microwave assisted NaOH activation, Chem. Eng. J., 187 (2012) 53–62.

[9] K.Y. Foo, B.H. Hameed, Microwave-assisted preparation and adsorption performance of activated carbon from biodiesel industry solid reside: influence of operational parameters, Bio. Technol., 103 (2012) 398–404.

[10] P. Liu, H.B. Wang, G.Z. Li, X.Y. Fang, Optimization of activation conditions of high-performance activated carbon from coffee shell by response surface methodology, Bio. Chem. Eng., 51 (2017) 43–47.

[11] K.Y. Foo, B.H. Hameed, Coconut husk derived activated carbon via microwave induced activation: effects of activation agents, preparation parameters and adsorption performance, Chem. Eng. J., 184 (2012) 57–65.

[12] K. Murashko, D. Nevstrueva, A. Pihlajamäki, T. Koiranen, J. Pyrhönen, Cellulose and activated carbon based flexible electrical double-layer capacitor electrode: preparation and characterization, Energy, 119 (2017) 435–441.

[13] K.G. Rekha, R. Radhika, T. Jayalatha, S. Jacob, R. Rajeev, B.K. George, Removal of perchlo-rate from drinking water using granular activated carbon modified by acidic functional group: adsorption kinetics and equilibrium studies, Proc. Safety Environ. Protect., 109 (2017) 158–171.

[14] H.C. Sariol, J. Maggen, J. Czech, G. Reekmans, G. Reggers, J. Yperman, Characterization of the exhaustion profile of activated carbon in industrial rum "filters" based on TGA, TD-GC/MS, colorimetry and NMR relaxometry, Mater. Today Commun., 11 (2017) 1–10.

[15] S.H.M. Arshad, N. Ngadi, A.A. Aziz, N.S. Amin, M. Jusoh, S. Wong, Preparation of activated carbon from empty fruit bunch for hydrogen storage, J. Energy Storage, 8 (2016) 257–261.

[16] L. Zhou, Impacts of the adsorptive storage of hydrogen on super activated carbons to large-scale utilization of hydrogen energy, Sci. Technol. Herald, 17 (1999) 10–11 (In Chinese).

[17] L. Zhan, K.X, Li, C.X. Lu, X. M. Zhu, Y. Song, L.C. Ling, The preparation of super activated carbons and its properties for hydrogen storage, New Carbon Mater., 20 (2001) 31–25.

[18] G. Li, J. Li, W. Tan, H. Jin, H. Yang, J. Peng, Preparation and characterization of the hydrogen storage activated carbon from coffee shell by microwave irradiation and KOH activation, Inter. Biodeterior. Biodegrad., 113 (2016) 386–390.

[19] X.Z. Sun, X. Zhang, D.C. Zhang, Y.W. Ma, Activated carbon-based super capacitors using Li_2SO_4 aqueous electrolyte, Acta Phys. Chim. Sin., 28 (2012) 367–372.

[20] Y.F. Liu, Tailoring pore size and surface modification of activated carbon as electrode materials for supercapacitor, Tongji University, 2008 (In Chinese).

[21] Z. Chen, Y.L. Zhang, H.T. Liu, Highly capacitance-enhanced activated carbons by oxidation-activation treatments for supercapacitor applications, J. Central South Univ., 43 (2012) 4638–4645.

[22] H.S. Song, Study on the preparation and properties of activated carbon electrode materials for supercapacitors, Central South Univ., 2007, (In Chinese).

[23] B. Conway, Electrochemical Supercapacitors Scientific Fundamentals and Technological Applications, Kluwer Academic, New York, 1996.

[24] Z. Zapata-Benabithe, G. Diossa, C.D. Castro, G. Quintana, Activated carbon bio-xerogels as electrodes for super capacitors applications, Procedia Eng., 148 (2016) 18–24.